Molecular Crystals and Liquid Crystals
Publication details, including instructions for authors and subscription information:
http://www.tandfonline.com/loi/gmcl20

Ultrafast All-Optical Switching with Transparent and Absorptive Nematic Liquid Crystals-Implications in Tunable Metamaterials

I. C. Khoo [a], J. Liou [a], M. V. Stinger [a] & Shuo Zhao [a]
[a] Electrical Engineering Department, Pennsylvania State University, University Park, PA, USA

Version of record first published: 14 Jun 2011

To cite this article: I. C. Khoo, J. Liou, M. V. Stinger & Shuo Zhao (2011): Ultrafast All-Optical Switching with Transparent and Absorptive Nematic Liquid Crystals-Implications in Tunable Metamaterials, Molecular Crystals and Liquid Crystals, 543:1, 151/[917]-159/[925]

To link to this article: http://dx.doi.org/10.1080/15421406.2011.569456

Mol. Cryst. Liq. Cryst., Vol. 543: pp. 151/[917]–159/[925], 2011

ISSN: 1542-1406 print/1563-5287 online
DOI: 10.1080/15421406.2011.569456

Taylor & Francis
Taylor & Francis Group

Ultrafast All-Optical Switching with Transparent and Absorptive Nematic Liquid Crystals–Implications in Tunable Metamaterials

I. C. KHOO, J. LIOU, M. V. STINGER, AND SHUO ZHAO

Electrical Engineering Department, Pennsylvania State University, University Park, PA, USA

We present a critical review of the nonlinear optical responses of nematic liquid crystals associated with short pulsed laser induced thermal, density and order parameter fluctuations. Experimental studies conducted with absorbing as well as transparent nematic liquid crystals have demonstrated that all-optical one-way switching of nanoseconds pulsed laser at 750 nm can be realized at sub-microseconds to nanoseconds speed. Similar switching performances have also been observed with lasers at other visible–infrared regime, confirming the broadband applicability of the underlying nonlinear optical processes.

Keywords Agile frequency laser hardening; all-optical switching; metamaterials; sensor protection; ultrafast; visible-infrared

1. Introduction

There have been intense research activities on micro- and nano-structures such as photonic crystals, and metamaterials owing to their potentials for novel optical functions [1–8]. To impart tuning capabilities to these materials/structures, nematic liquid crystals have frequently been employed owing to their unique physical and optical properties [9]. Most reported experimental studies employ ac electric field induced director axis reorientation or temperature-controlled birefringence modification [5,7]. These mechanisms are generally slow, with switching times ranging on the order of tens of milliseconds to seconds. Nonlinear all-optical or self-action mechanisms, in which the desired changes in optical refractive indices or birefringence are generated by the light intensity itself, are clearly more preferable since they do not require any electrode, and the incident light can impinge at almost any angle desired. In these regards, nematic liquid crystals also stand out as a highly promising candidate owing to their extraordinarily large nonlinear optical responses arising from a multitude of mechanisms [9,10]. Almost all nonlinear

Address correspondence to I. C. Khoo, Electrical Engineering Department, Pennsylvania State University, University Park, PA 16802, USA. Tel.: 814-863-2299; Fax: 814-865-7065; E-mail: ick1@psu.edu

optical processes have been observed, in conjunction with a wide spectrum of lasers. The responses time of such optically induced effects generally can be made much shorter by virtue of the intensity dependence of these processes, as exemplified in various studies involving sub-milliseconds–nanoseconds as well as picoseconds laser pulses [10–18].

In this paper, we present a theoretical analysis and experimental feasibility demonstration of a particular self-action switching action with sub-microseconds–nanoseconds response times, that may be useful for developing tunable metamaterials and other materials/structures impregnated with nematic liquid crystals. The underlying mechanism – laser induced birefringence modification – could also enable faster-response version of many coherent optical image processing applications demonstrated previously with slower mechanisms [10,19–22].

2. Theoretical Analysis

Figure 1 depicts a typical optical switching configuration involving a 90° twist-alignment nematic liquid crystal placed between two crossed polarizers [17,18]. In the absence of any applied field, or when the incident light intensity is not strong enough to perturb the nematic order/birefringence, the incident light polarization follows the director axis rotation and emerges on the exit side with its polarization along the exit polarizer's, i.e., maximum transmission.

In the layered transfer matrix formalism [18], the amplitude of the normalized transmitted light through the liquid crystal cell (between polarizers) is given by:

$$\Psi_{out}(d) = \begin{pmatrix} E'_x \\ E'_y \end{pmatrix} = P(\phi_{Exit}) \cdot \prod_{m=1}^{M} [S^{-1}(\phi_m) \cdot G \cdot S(\phi_m)] \cdot \begin{pmatrix} \cos\phi_{Ent} \\ \sin\phi_{Ent} \end{pmatrix} \quad (1)$$

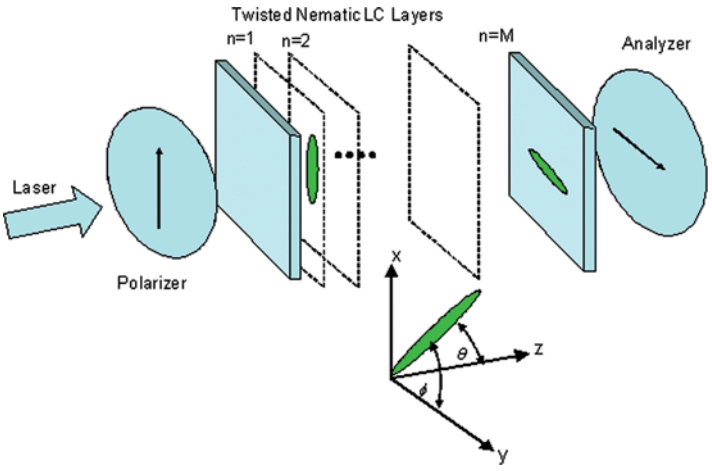

Figure 1. Schematic depiction of the propagation of a linearly polarized light through a 90° twist alignment nematic liquid crystal cell for the modified Jones matrix calculation. (Figure appears in color online.)

$$P(\phi) = \begin{pmatrix} \cos^2\phi & \cos\phi\sin\phi \\ \sin\phi\cos\phi & \sin^2\phi \end{pmatrix}; \quad S(\phi_m) = \begin{pmatrix} \cos\phi_m & \sin\phi_m \\ -\sin\phi_m & \cos\phi_m \end{pmatrix};$$
$$G = \begin{pmatrix} e^{i\frac{\gamma}{2}} & 0 \\ 0 & e^{-i\frac{\gamma}{2}} \end{pmatrix} \tag{2}$$

$$\gamma = \frac{2\pi h \Delta n_m}{\lambda}; \Delta n_m = \frac{n_e n_o}{\sqrt{n_e^2 \sin^2\theta_m + n_o^2 \cos^2\theta_m}} - n_o \tag{3}$$

Here γ is the retardation (or phase shift) associated with the birefringence Δn_{m} of the *m-th* LC layer, θ_m and φ_{m} are the tilt and twist angle of *m*-th layer director axis and ϕ_{Ent},ϕ_{Exit} are the axis of the entrance polarizer and exit analyzer, respectively (e.g., $\phi_{Ent} = 90^\circ$ and $\phi_{Exit} = 0^\circ$).

The key to optical switching is the retardation γ imparted by the liquid crystal film. The birefringence of the layer at any time t is strongly dependent on the local order parameter S, i.e., Δn_m (t) = Δn (S). The order parameter is in turn dependent on the local temperature and density fluctuations [ΔT(t) and $\Delta\rho$(t)], as well as the number density $\Delta \mathrm{N_c}$(t) of laser–excited Cis-species that impart local disorder, c.f. Figure 2a–b, respectively. Accordingly, Δn_m (t) = Δn (S; ΔT, $\Delta\rho$, $\Delta \mathrm{N_c}$). In conventional electro-optics switches, an applied ac field realigns the director axis and diminishes the birefringence with a characteristics response time of several milliseconds. On the other hand, all-optical switching is mediated by changing the birefringence through the aforementioned temperature, density and other disorder mechanisms, and could take place at faster rates.

Consider for example the case of birefringence modification associated with laser induced temperature and order parameter changes. In the Landau-deGennes formalism, the free energy of the nematic system is described by the following expression [18]:

$$f(S(z)) = a(T(z) - T^*)S(z)^2 + BS(z)^3 + CS(z)^4 + L\left(\frac{dS(z)}{dz}\right)^2 - G_1S_1 - G_2S_2 \tag{4}$$

Recall here the relationships between the refractive indices and the nematic birefringence and the order parameter ***S*** and the density ρ [9,23]:

$$n_{\parallel}^2 = 1 + \left(\frac{N}{3\varepsilon_0}\right)[\alpha_l K_l(2S+1) + \alpha_t K_t(2-2S);$$
$$n_{\perp}^2 = 1 + \left(\frac{N}{3\varepsilon_0}\right)[\alpha_l K_l(1-S) + \alpha_t K_t(2+S)$$

$$\Delta\varepsilon = n_{\parallel}^2 - n_{\perp}^2 = \left(\frac{N}{3\varepsilon_0}\right)[\alpha_l K_l - \alpha_t K_t]S = \frac{N_A\rho}{\varepsilon_0 M}(\alpha_l K_l - \alpha_t K_t) \sim \rho S \tag{5}$$

Here K_l and K_t are the values of local field correction tensor $\overrightarrow{\overrightarrow{K}}$ components along/perpendicular to the principal axis, respectively, and other material parameters are defined in the literature [9,23]. Clearly, the birefringence of the nematic ($\Delta n = n_{\parallel} - n_{\perp}$) is a very strongly coupled function of the temperature *T*, density ρ and the order

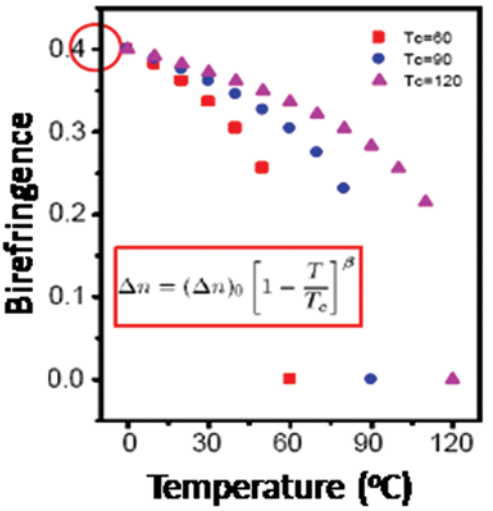

(a)

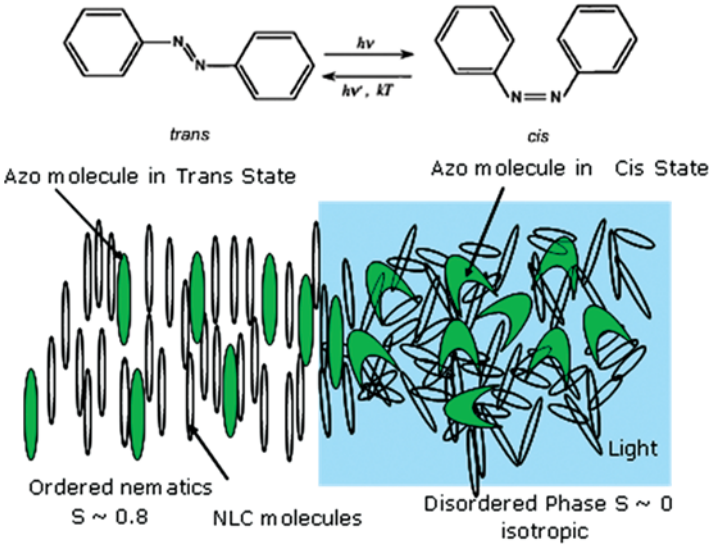

(b)

Figure 2. (a): Temperature dependence of the birefringence Δn of nematics with different phase transition temperatures T_c; (b): Schematic depiction of disorder caused by laser induced trans-cis conformational changes of the azo-molecules in an initially aligned nematic liquid crystal. (Figure appears in color online.)

parameter S. For a given (fixed) director axis orientation, the laser induced temperature (ΔT) and density ($\Delta\rho$) changes are described by the following coupled hydrodynamical equations [13,28]:

$$-\frac{\partial^2}{\partial t^2}(\Delta\rho) + v^2\nabla^2(\Delta\rho) + v^2\beta_T\rho_0\nabla^2(\Delta T) + \frac{\eta}{\rho_0}\frac{\partial}{\partial t}\nabla^2(\Delta\rho) = \frac{\gamma^e}{8\pi}\nabla^2(E^2) \qquad (6a)$$

$$\rho_0 C_v \frac{\partial}{\partial t}(\Delta T) - \lambda_T \nabla^2(\Delta T) - \frac{(C_p - C_v)}{\beta_T}\frac{\partial}{\partial t}(\Delta\rho) = \frac{u}{\tau} = \frac{\alpha nc}{4\pi}E^2 \tag{6b}$$

Here ρ_0 is the unperturbed density of the liquid crystal, C_p and C_v the specific heats, λ_T the thermal conductivity, η the viscosity, v the speed of sound, γ^e the electrostrictive coefficient [$\gamma^e = \rho_0(\rho\varepsilon/\partial\rho)_T$], β_T the coefficient of volume expansion, and η a viscosity coefficient; E is the amplitude of the laser optical electric field strength.

The driving term on the right hand side of equations (6a) arises from electrostriction (movement of materials toward strong field region) generated by the large field gradient of tightly focused lasers. This mechanism can occur in all (including transparent) materials. In (6b), the driving term is photo-absorption and the resulting heating and thermal expansion. The response times associated with these laser induced temperature and density changes, and the resulting order parameter and the birefringence modifications are in general dependent on the rate of laser absorption and characteristic diffusion lengths. For short intense laser pulses, the on-time (time needed to achieve the required phase shift) can be as short as several nanoseconds. On the other hand, for characteristics diffusion length on the order of tens of microns, the typical thermal- and density relaxation- times constant are microseconds and nanoseconds, respectively [9,23].

To illustrate the dynamics of such switching process, we present here a theoretical simulation of laser induced thermal effects associated with a Gaussian laser pulse, using typical nematic parameters. Figure 3 depicts the typical temporal characteristics of the input and output laser pulses for various input energy levels that are high

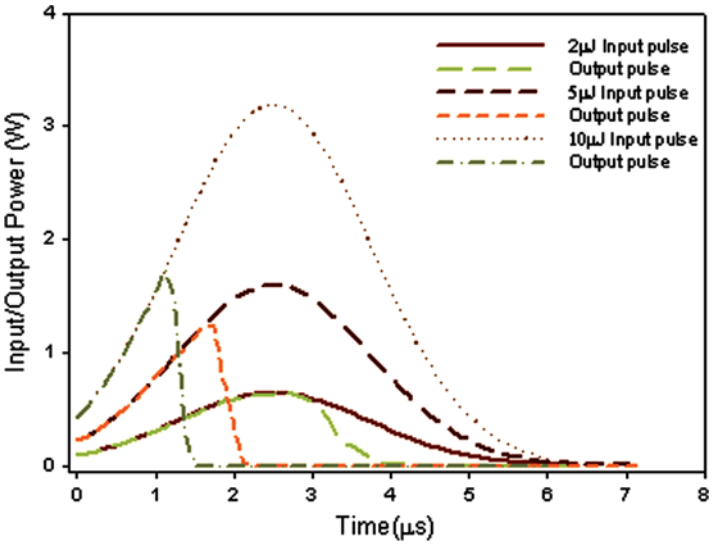

Figure 3. Theoretical simulation of the output and input pulses for various laser pulse energies exhibiting shorter switching times with increasing laser energies. Parameters used are: $Cp = Cv = 2300\,J/(kg * K)$; thermal conductivity $\lambda_T = 0.15\,W/(m * K)$; $\rho = [1.4139 - 17.7 \times 10^{-4}\,T + 1.484 \times 10^{-6}\,T^2] \times 10^3\,kg/m^3$; $\alpha = 2 \times 10^4/m$ (initial linear transmission ~70%); sample thickness: 20 μm; laser spot diameter: 40 μm; ambient temperature $T = 300^\circ$ K.

enough to cause transmission switching. In the first 50 nanoseconds or so when the cumulative absorbed laser energy is not sufficient to effect significant temperature/order parameter changes, the output pulse follows the input in an almost linear fashion. At later times, when the deposited laser energies are substantial, the transmission begins to drop dramatically, and diminishes to almost vanishing value in a switch-off time τ_{off} that becomes shorter (from $\sim$1 μs to $\sim$100 ns) as the laser input energy fluence is increased from $\sim 2\,\mu J/(40\,\mu m)^2$ to $\sim 10\,\mu J(40\,\mu m)^2$; at higher input laser fluence and/or absorption constant, the switching times becomes even shorter, approaching a few nanoseconds in sample of similar thicknesses and initial transmission.

3. Nonlinear Ultrafast Transmission Switching in Dyed and Transparent Nematic Cells

We have studied such optical switching processes with IR-78 doped nematic liquid crystals (5CB). Besides 'thin' sample-thicknesses of $\sim$20 μm to 50 μm, we have also studied the responses of thick samples (>100 μm). 90°-twist alignment cells are made by filling two orthogonally rubbed PVA-coated glass windows. [Note: to assess only the contribution from laser absorption, and to exclude scattering/reflection losses, the transmission values quoted here refer to the doped and undoped 5CB in the isotropic phase]. For the doped samples, the linear transmission at 750 nm at low input laser power is in the range of 30−70%. We have also studied undoped (transparent) samples with an initial transmission of nearly 99%. The laser used is a Q-switched Alexandrite laser operating at 750 nm and a pulse-duration of 250 ns. Depending on the placement of the nematic cell from the focal plane, the laser focal spot diameter on the sample is in the range from 120–140 μm.

As expected, at low input laser power/energy (<1 μJ), the output is linearly related to the input pulse in its magnitude and temporal characteristics. On the other hand, at input laser energy above $\sim$10 μJ, dramatic decreases in the transmission are manifested in later portion of the output pulse, c.f. photo insert in Figure 4, in very good agreement with theoretical simulation. The time it takes to diminish to vanishing transmission value grows shorter as the input laser energy fluence is increased; we have observed switch-off times as short as 25 nanoseconds. Such clamping and faster switching-off action on the later portion of the pulse gives rise to a net transmission (total transmitted laser energy/input energy) that continues to drop as the incident laser energy is raised. For the switching set up, the ultimate extinction ratio is dictated by the crossed input/exit polarizers used, which is measured to be $\sim 10^{-3}$ in this case.

Similar results have been observed in thicker samples. Figure 5 shows the results obtained with doped samples of two different concentrations (0.09% and 0.13%) and two thicknesses (130 μm and 150 μm), and a 150-μm thick transparent sample. As expected, the thresholds for switching to manifest in doped samples are generally lower for higher dye-doping or thicker samples, with the corresponding shortening of the switch-off times [not shown]. A particularly interesting, and potentially very useful observation comes from the non-absorbing sample, where similar all-optical switching effects are also manifested. The transmission switching occurs at comparable threshold (a few μJ) with similar dependence on the input energy. Discounting thermal effects, the underlying mechanism is attributed to laser induced electrostriction, which causes material flows and consequently density changes as well as

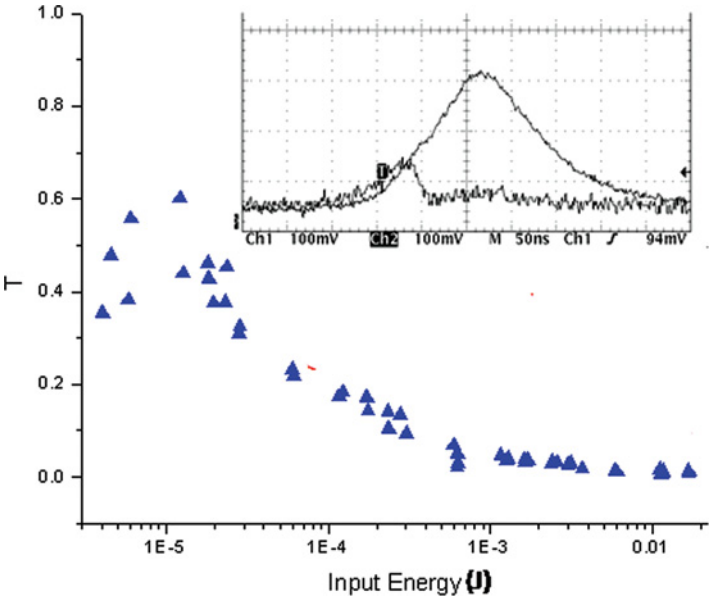

Figure 4. Experimental results for the nonlinear transmission as a function of the input laser energy of a 30 μm-thick nematic cell with 0.1% dye (initial linear transmission of 70%). Photo insert shows the input (upper trace) and output laser pulses at high input energy when significant transmission switching is detected. (Figure appears in color online.)

director axis randomization and disorder, similar to previously observed high frequency acoustic waves and flow effects with visible ($\lambda = 532$ nm) pulsed lasers [11,24–26]. The high initial linear transmission state of these transparent nematic

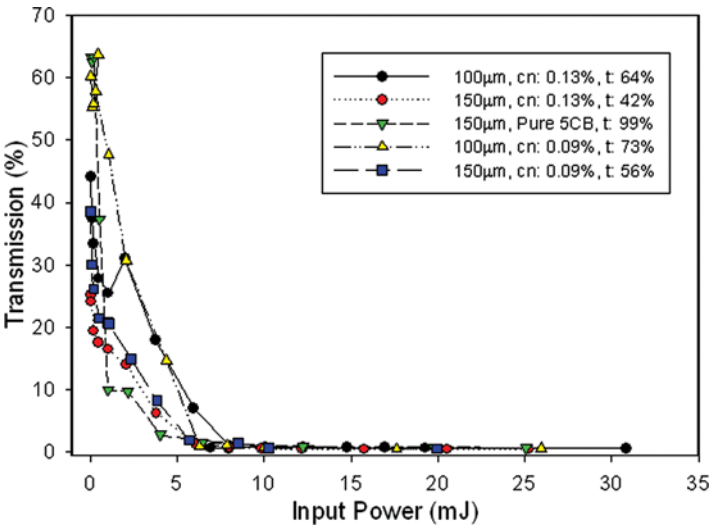

Figure 5. Experimental results for the transmission of a 0.25 μs laser pulse through various doped and pure (transparent) nematic cell.

cells and the wavelength independence of the mechanism make them attractive features for switching and limiting operations against agile frequency pulsed lasers.

4. Conclusion

We have presented a theoretical account and experimental demonstration of ultrafast all-optical switching in absorbing as well as transparent nematic liquid crystals, attributable to laser induced thermal/density fluctuations, flow and order parameter modifications. For a typical configuration involving a twist-alignment nematic cell placed between crossed-polarizers, very high extinction one-way switching can be realized with switch-off times as short as nanoseconds. These effects could be useful for broadband agile frequency laser hardening and optical sensor protection application, as well as for imparting electrode-free tuning capabilities to nanostructures and metamaterials with nematic constituents. We have repeated these observations with lasers at various visible–near infrared regimes (488 nm, 532 nm, 1060 nm, 1550 nm) and observed similar performance. Detailed theoretical and experimental studies are currently underway and the results will be presented in longer articles elsewhere.

Acknowledgment

This work is supported by the Air Force Office of Scientific Research, the Army Research Office and the National Science Foundation Material Research Science and Engineering Center DMR-0820404.

References

[1] Fang, N., Lee, H., Sun, C., & Zhang, X. (2005). *Science*, *308*, 534–537.
[2] Shalaev, V. M., Cai, W. S., Chettiar, U. K., Yuan, H. K., Sarychev, A. K., Drachev, V. P., & Kildeshev, A. V. (2005). *Opt. Letts.*, *30*, 3356–3358.
[3] Khoo, I. C., Werner, D. H., Liang, X., & Diaz, A. (2006). *Opt. Lett.*, *31*, 2592.
[4] Werner, D.-H., Kwon, D.-H., Khoo, I. C., Kildeshev, A. K., & Shalaev, V. M. (2007). *Optics Express*, *15*(6), 3342–3347.
[5] Graugnard, E., King, J. S., Jain, S., Summers, C. J., Zhang-Williams, Y., & Khoo, I. C. (2005). *Phys. Rev. B*, *72*, 233105.
[6] Zhao, Q., Kang, L., Du, B., Li, B., Zhou, J., Tang, H., Liang, X., & Zhang, B. Z. (2007). *Appl. Phys. Lett.*, *90*, 011112.
[7] Xiao, Shumin, Chettiar, Uday K., Kildishev, Alexander V., Drachev, Vladimir, Khoo, I. C., & Shalaev, Vladimir M. (2009). *Appl. Phys. Lett.*, *95*(3), 033115.
[8] Khoo, I. C., Diaz, A., Liou, J., Stinger, M. V., Huang, J., & Ma, Y. (2010). *IEEE J., Selected Topics in Quantum Electronics*, Special Issue *16*, 410–417.
[9] Khoo, I. C. (2007). "*Liquid Crystals*", 2nd Edition, Wiley Inter-Science: NJ.
[10] Khoo, I. C. (2009). *Physics Report*, *471*, 221–267.
[11] Khoo, I. C., Lindquist, R. G., Michael, R. R., Mansfield, R. J., & Lopresti, P. (1991). *J. Appl. Phys.*, *69*, 3853.
[12] Li, Hong, Liang, Yu, & Khoo, I. C. (1994). *Mol. Cryst. Liq. Cryst.*, *251*, 85.
[13] Khoo, I. C., Finn, G., Michael, R. R., & Liu, T. H. (1986). *Optics Letters*, *11*, 227–229.
[14] Khoo, I. C., & Li, H. (1994). *Appl. Phys. B*, *59*, 573.
[15] Khoo, I. C. (1996). *Mol. Cryst. Liq. Cryst.*, *282*, 53–66.
[16] Khoo, I. C., & Shepard, S. (1983). *J. Appl. Phys.*, *54*, 5491.

[17] Khoo, I. C., Park, Jae-Hong, & Liou, Justin (2007). *Appl. Phys. Letts.*, *90*, 151107.
[18] Khoo, I. C., Park, J. H., & Liou, J. D. (2008). *J. Opt. Soc. Am. B*, *25*, 1931–1937.
[19] Shih, M. Y., Shishido, A., & Khoo, I. C. (2001). *Opt. Letts.*, *26*, 1140–1142.
[20] Khoo, I. C., & Liang, Y. (2000). *Phys. Rev. E*, *62*, 6722–6733.
[21] Shih, M. Y., Khoo, I. C., Shishido, A., Wood, M. V., & Chen, P. H. (2000). *Opt. Letts.*, *25*, 978–980.
[22] Khoo, I. C., & Zhuang, S. L. (1981). *IEEE J. Quant. Electronics*, *QE-18*, 246–249.
[23] Khoo, I. C., & Normandin, R. (1985). *IEEE J. Quant. Electronics*, *QE-21*, 329.
[24] Khoo, I. C., Michael, R. R., & Yan, P. Y. (1987). IEEE J. Quant. Electronics, *QE23*, 267.
[25] Khoo, I. C., & Normandin, R. (1984). *Opt. Letts.*, *9*, 285–287.
[26] Eichler, H. J., & Macdonald, R. (1991). *Phys. Rev. Letts.*, *67*, 2666–2668.